Biogeosciences, 17, 1309–1326, 2020
https://doi.org/10.5194/bg-17-1309-2020

Biogeosciences Open Access EGU

Experiment design and bacterial abundance control extracellular H_2O_2 concentrations during four series of mesocosm experiments

Mark J. Hopwood[1], Nicolas Sanchez[2], Despo Polyviou[3], Øystein Leiknes[2], Julián Alberto Gallego-Urrea[4], Eric P. Achterberg[1], Murat V. Ardelan[2], Javier Aristegui[5], Lennart Bach[6], Sengul Besiktepe[7], Yohann Heriot[1], Ioanna Kalantzi[8], Tuba Terbıyık Kurt[9], Ioulia Santi[8], Tatiana M. Tsagaraki[10], and David Turner[11]

[1]GEOMAR Helmholtz Centre for Ocean Research Kiel, Kiel, Germany
[2]Norwegian University of Science and Technology, Trondheim, Norway
[3]Ocean and Earth Science, National Oceanography Centre Southampton, Southampton, UK
[4]Department of Marine Sciences, Kristineberg Marine Research Station, University of Gothenburg, Gothenburg, Sweden
[5]Instituto de Oceanografía y Cambio Global, IOCAG, Universidad de Las Palmas de Gran Canaria, ULPGC, Las Palmas, Spain
[6]Institute for Marine and Antarctic Studies, University of Tasmania, Hobart, Tasmania, Australia
[7]The Institute of Marine Sciences and Technology, Dokuz Eylul University, Izmir, Turkey
[8]Institute of Oceanography, Hellenic Centre for Marine Research, Heraklion, Greece
[9]Department of Marine Biology, Faculty of Fisheries, Çukurova University, Adana, Turkey
[10]Department of Biological Sciences, University of Bergen, Bergen, Norway
[11]Department of Marine Sciences, University of Gothenburg, Gothenburg, Sweden

Correspondence: Mark J. Hopwood (mhopwood@geomar.de)

Received: 25 May 2018 – Discussion started: 20 June 2018
Revised: 24 November 2019 – Accepted: 29 November 2019 – Published: 16 March 2020

Abstract. The extracellular concentration of H_2O_2 in surface aquatic environments is controlled by a balance between photochemical production and the microbial synthesis of catalase and peroxidase enzymes to remove H_2O_2 from solution. In any kind of incubation experiment, the formation rates and equilibrium concentrations of reactive oxygen species (ROSs) such as H_2O_2 may be sensitive to both the experiment design, particularly to the regulation of incident light, and the abundance of different microbial groups, as both cellular H_2O_2 production and catalase–peroxidase enzyme production rates differ between species. Whilst there are extensive measurements of photochemical H_2O_2 formation rates and the distribution of H_2O_2 in the marine environment, it is poorly constrained how different microbial groups affect extracellular H_2O_2 concentrations, how comparable extracellular H_2O_2 concentrations within large-scale incubation experiments are to those observed in the surface-mixed layer, and to what extent a mismatch with environmentally relevant concentrations of ROS in incubations could influence biological processes differently to what would be observed in nature. Here we show that both experiment design and bacterial abundance consistently exert control on extracellular H_2O_2 concentrations across a range of incubation experiments in diverse marine environments.

During four large-scale (> 1000 L) mesocosm experiments (in Gran Canaria, the Mediterranean, Patagonia and Svalbard) most experimental factors appeared to exert only minor, or no, direct effect on H_2O_2 concentrations. For example, in three of four experiments where pH was manipulated to 0.4–0.5 below ambient pH, no significant change was evident in extracellular H_2O_2 concentrations relative to controls. An influence was sometimes inferred from zooplankton density, but not consistently between different incubation experiments, and no change in H_2O_2 was evident in controlled experiments using different densities of the copepod *Calanus finmarchicus* grazing on the diatom *Skeletonema costatum* (< 1 % change in $[H_2O_2]$ comparing copepod densities from 1 to 10 L^{-1}). Instead, the changes in H_2O_2 concentration contrasting high- and low-zooplankton incubations appeared to arise from the resulting changes in bac-

terial activity. The correlation between bacterial abundance and extracellular H_2O_2 was stronger in some incubations than others (R^2 range 0.09 to 0.55), yet high bacterial densities were consistently associated with low H_2O_2. Nonetheless, the main control on H_2O_2 concentrations during incubation experiments relative to those in ambient, unenclosed waters was the regulation of incident light. In an open (lidless) mesocosm experiment in Gran Canaria, H_2O_2 was persistently elevated (2–6-fold) above ambient concentrations; whereas using closed high-density polyethylene mesocosms in Crete, Svalbard and Patagonia H_2O_2 within incubations was always reduced (median 10 %–90 %) relative to ambient waters.

1 Introduction

Reactive oxygen species (ROSs), such as H_2O_2, are ubiquitous in surface aquatic environments due to photochemical formation (Van Baalen and Marler, 1966; Moore et al., 1993; Miller and Kester, 1994). Quantum yields for H_2O_2 formation increase with declining wavelength and so the ultraviolet (UV) portion of natural sunlight is a major source of H_2O_2 in surface aquatic environments (Cooper et al., 1988, 1994). Sunlight-normalized H_2O_2 production rates therefore peak between wavelengths of 310 and 340 nm (Kieber et al., 2014). H_2O_2 is present at concentrations on the order of 10–100 nM in the ocean's surface mixed layer with its concentration generally declining sharply with depth (Price et al., 1998; Yuan and Shiller, 2001; Gerringa et al., 2004). Because its decay rate is slow (observed half-lives in seawater range from 10 to 120 h; Petasne and Zika, 1997) compared to less stable ROSs such as superoxide ($O_2^{\cdot-}$) and the hydroxyl radical ($OH^{\cdot}$), extracellular H_2O_2 concentrations in surface waters show a pseudo-sinuous diurnal cycle, with elevated H_2O_2 concentrations occurring during daylight hours (Price et al., 1998). In addition to photochemical generation of ROS in the photic zone, there is also extensive evidence of dark formation processes for H_2O_2 in both surface and subsurface waters (Palenik and Morel, 1988; Vermilyea et al., 2010; Roe et al., 2016).

H_2O_2 features as a reactive intermediate in the natural biogeochemical cycling of many compound groups including halocarbons (Hughes and Sun, 2016), trace metals (Moffett and Zika, 1987; Voelker and Sulzberger, 1996; Hansel et al., 2015) and dissolved organic matter (DOM) (Cooper et al., 1988; Scully et al., 2003). Previous work has highlighted the susceptibility of a broad range of marine biota to elevated extracellular H_2O_2 concentrations (Bogosian et al., 2000; Morris et al., 2011) and argued that measurable negative effects on metabolism occur in some marine species at H_2O_2 concentrations within the range of ambient surface and mixed-layer concentrations (Morris et al., 2011; Baltar et al., 2013). Peroxidase and catalase enzymes are widely produced by marine microbes to lower extracellular H_2O_2 concentrations, and these enzymes are the dominant sink for H_2O_2 in the surface marine environment (Moffett and Zafiriou, 1990; Angel et al., 1999). Although many community members possess the ability to enzymatically remove extracellular H_2O_2, they may not actively express this ability constantly, with H_2O_2 defences thought to be subject to diurnal regulation (Morris et al., 2016). The reliance of some species including strains of *Prochlorococcus*, which do not produce such enzymes, on other "helper" organisms to remove extracellular H_2O_2 underpins a theory of reductive evolution, "the Black Queen Hypothesis" (BQH) (Morris et al., 2012). BQH infers that because the removal of extracellular H_2O_2 by any species is a communal benefit, there is an energetic benefit to be gained by an individual species by losing genes associated with extracellular H_2O_2 detoxification. Loss of these genes continues to be favourable to individual species until only a minority of community members poses the ability to remove H_2O_2, and the benefit of further loss would be offset by the negative effects of increasing extracellular H_2O_2 concentrations (Morris et al., 2012).

It is already acknowledged that laboratory incubation studies using buffered growth media are often conducted at H_2O_2 concentrations 2–10 times higher than those found in the surface ocean (Morris and Zinser, 2013). We have previously hypothesized that the same may be generally true for mesoscale experiments (Hopwood et al., 2018) because the relative stability of H_2O_2 means that the enclosure of water at the ocean's surface within mesocosms can lead to elevated H_2O_2 concentrations. Yet there are presently few examples in the literature of incubation experiments where ROS concentrations are measured, and therefore it is unknown how changes to other stressors, or changes to experimental design, affect extracellular ROS concentrations. In order to assess whether ROS could be a significant artefact in incubation experiments, and to investigate how extracellular H_2O_2 concentrations respond to changes in DOC, pH, ambient light and grazing pressure, here we collate data on H_2O_2 from a series of small- to large-scale (20–8000 L) incubation experiments with varying geographical location (Table 1).

2 Methods

Our rationale for the investigation of H_2O_2 trends during these 20–8000 L scale mesocosm and microcosm experiments is that the experiment matrixes for each experiment permitted the changing of 1, 2 or 3 key variables (DOC, zooplankton, pH) whilst maintaining others (e.g. salinity, temperature, light) in a constant state across the mesocosm–microcosm experiment. The relationships between H_2O_2 and other chemical–biological parameters are therefore potentially easier to investigate than in the ambient water column where mixing and the vertical–lateral trends in H_2O_2 concentrations must also be considered. Additionally, two of the

Table 1. Experiment details for each experiment. For a visual representation of experiment designs, the reader is referred to the Supplement. "HDPE" denotes high-density polyethylene. "n/a" denotes "not applicable".

Experiment	PAT (Patagonia)	ARC (Svalbard, Arctic)	MED (Crete, Mediterranean)	Gran Canaria
Mesocosm	*MesoPat*	*MesoArc*	*MesoMed*	*Gran Canaria*
Containers	HDPE 1000 L	HDPE 1250 L	HDPE 1500 L	Polyurethane 8000 L
Design (Fig. S1, Supplement)	I	I	I	IV
Location	Comau fjord, in situ	Kongsfjorden, Svalbard, in situ	Hellenic Centre for Marine Research, Crete, temperature-controlled pool	Taliarte Harbour, in situ
Month/year	November 2014	July 2015	May 2016	March 2016
Duration (days)	11	12	12	28
Lighting	Ambient	Ambient	Ambient reduced $\sim 50\,\%$ with net	Ambient
Zooplankton treatment	$+30$ copepods L^{-1}	$+5$ copepods L^{-1}	$+4$ copepods L^{-1}	n/a
Macronutrient addition	N added as NO_3	N added as NH_4	N added as 50/50 NH_4/NO_3	N added as NO_3
Macronutrient addition timing	Daily	Daily	Daily	Day 18 only
Macronutrients added (per addition)	1.0 µM NO_3, 1.0 µM Si, 0.07 µM PO_4	1.12 µM NO_3, 1.2 µM Si, 0.07 µM PO_4 (11.4 µM Si added on day 1)	48 nM NO_3, 48 nM NH_4, 6 nM PO_4	3.1 µM NO_3, 1.5 µM Si, 0.2 µM PO_4
Screening of initial seawater	n/a	200 µm	140 µm	3 mm
Multistressor	*MultiPat*	*MultiArc*	*MultiMed*	
Containers	HDPE collapsible 20 L	HDPE collapsible 20 L	HDPE collapsible 20 L	
Design (Fig. S1)	II	II	II	
Location	Comau fjord, temperature-controlled room	Kongsfjorden, Svalbard, temperature-controlled room	Hellenic Centre for Marine Research, Crete, temperature-controlled room	
Month/year	November 2014	July 2015	May 2016	
Duration (days)	8	8	9	
Lighting	36 W lamps	36 W lamps	36 W lamps	
Light regime	15 h light, 9 h dark	24 h light	15 h light, 9 h dark	
Zooplankton treatment	$+30$ copepods L^{-1}	$+5$ copepods L^{-1}	$+4$ copepods L^{-1}	
Macronutrient addition	Same as MesoPat	Same as MesoArc	Same as MesoMed	
Macronutrient addition timing	Daily	Daily	Daily	
Macronutrients added (per addition)	1.0 µM NO_3, 1.0 µM Si, 0.07 µM PO_4	1.12 µM NH_4, 1.2 µM Si, 0.07 µM PO_4	48 nM NO_3, 48 nM NH_4, 6 nM PO_4	
C added	0, 0.5, 1, 2 and $3\times$ Redfield	0, 0.5, 1, 2 and $3\times$ Redfield	0, 0.5, 1, 2 and $3\times$ Redfield	
pH post-adjustment	7.54 ± 0.09	7.76 ± 0.03	7.64 ± 0.02	
pH pre-adjustment	7.91 ± 0.01	8.27 ± 0.18	8.08 ± 0.02	

Table 1. Continued.

Experiment	PAT (Patagonia)	ARC (Svalbard, Arctic)	MED (Crete, Mediterranean)	Gran Canaria
Screening of initial seawater	200 µm	200 µm	140 µm	
Temperature (°C)	13–18	4.0–7.0	19.9–21.5	
Microcosm	*MicroPat*			
Containers	HDPE collapsible 20 L			
Design (Fig. S1)	III			
Location	Comau fjord, temperature controlled room			
Month/year	November 2014			
Duration (days)	11			
Lighting	36 W lamps			
Light regime	15 h light, 9 h dark			
Containers	HDPE collapsible 20 L			
Grazing treatment	+30 copepods L^{-1}			
Macronutrient addition timing	Daily			
Macronutrient addition	N was added as NO_3			
Macronutrients added (per addition)	1.0 µM NO_3, 1.0 µM Si, 0.07 µM PO_4			
Screening of initial seawater	200 µm			
Temperature (°C)	14–17			

experiment designs described herein (see Table 1) were repeated in three geographic locations facilitating direct comparisons between the experiment results with only limited mitigating factors concerning method changes.

2.1 Mesocosm set-up and sampling

Eight incubation experiments (Table 1) were constructed using coastal seawater which was either collected through pumping from small boats deployed offshore or from the end of a floating jetty. Three of these incubations were outdoor mesocosm experiments (MesoPat, MesoArc and MesoMed) conducted using the same basic set-up (based on that used in earlier experiments described by Larsen et al. (2015). For these three mesocosms, 10 identical cubic high-density polyethylene (HDPE) 1000–1500 L tanks were filled ∼ 95 % with seawater which was passed through nylon mesh (size as per Table 1) to remove mesozooplankton. The 10 closed mesocosm tanks were then held in position with a randomized treatment configuration and incubated at ambient seawater temperature. For MesoPat and MesoArc the mesocosms were tethered to a jetty. For MesoMed the mesocosms were held in a pool facility at the Hellenic Centre for Marine Research which was continuously flushed with seawater to maintain a constant temperature. An extra HDPE container (to which no additions were made) was also filled to provide an additional supply of un-manipulated seawater (without zooplankton, DOC or nutrient additions) for calibration purposes and baseline measurements on day 0. During MesoMed, this surplus container was incubated alongside the mesocosms for the duration of the experiment without any further additions or manipulation.

The 10-mesocosm experiment design matrix was the same for MesoPat, MesoArc and MesoMed (Fig. S1 in the Supplement, design I). For these three mesocosm experiments, zooplankton were collected 1 d in advance of requirement using horizontal tows at ∼ 30 m depth with a mesh net equipped with a non-filtering cod end. Collected zooplankton were then stored overnight in 100 L containers and non-viable individuals removed by siphoning prior to making

zooplankton additions to the mesocosm containers. After filling the mesocosms, zooplankton (quantities as per Table 1) were then added to five of the containers to create contrasting high- and low-grazing conditions. Macronutrients (NO_3/NH_4, PO_4 and Si) were added to mesocosms daily (Table 1). Across both the five high- and five low-grazing tank treatments, a dissolved organic carbon (DOC) gradient was created by addition of glucose to provide carbon at 0, 0.5, 1, 2 and 3 times the Redfield ratio (Redfield, 1934) with respect to added PO_4. Mesocosm water was sampled through silicon tubing (permanently fixed into each mesocosm lid) immediately after mixing of the containers using plastic paddles (also mounted within the mesocosms through the lids) with the first 2 L discarded in order to flush the sample tubing.

A fourth outdoor mesocosm experiment (Gran Canaria) used eight cylindrical polyurethane bags with a depth of approximately 3 m, a starting volume of ~ 8000 L and no lid or screen on top (Hopwood et al., 2018). After filling with coastal seawater the bags were allowed to stand for 4 d. A pH gradient across the eight tanks was then induced (on day 0) by the addition of varying volumes of filtered, pCO_2-saturated seawater (resulting in pCO_2 concentrations from 400 to 1450 µatm, treatments outlined Fig. S1 IV) using a custom-made distribution device (Riebesell et al., 2013). A single macronutrient addition (3.1 µM nitrate, 1.5 µM silicic acid and 0.2 µM phosphate) was made on day 18 (Table 1).

2.2 Microcosm and multistressor set-up and sampling

A 10-treatment microcosm (MicroPat) incubation mirroring the MesoPat 10 tank mesocosm (treatment design as per Fig. S1 I, but with 6×20 L containers per treatment – one for each time point – rather than a single HDPE tank) and three 16-treatment multistressor experiments (MultiPat, MultiArc and MultiMed Fig. S1 II) were conducted using artificial lighting in temperature-controlled rooms (Table 1, Fig. S1). For all three multistressor incubations (MultiPat, MultiArc and MultiMed) and the single microcosm incubation (MicroPat), coastal seawater (filtered through nylon mesh) was used to fill 20 L HDPE collapsible containers. The 20 L containers were arranged on custom-made racks with light provided by a network of 36 W lamps (Phillips, MASTER TL-D 90 De Luxe 36W/965 tubes). The number and orientation of lamps was adjusted to produce a light intensity of 80 µmol quanta m^{-2} s^{-1}. A diurnal light regime representing spring–summer light conditions at each field site was used, and the tanks were agitated daily and after any additions (e.g. glucose, acid or macronutrient solutions) in order to ensure a homogeneous distribution of dissolved components. In all 20 L scale experiments, macronutrients were added daily (as per Table 1). One 20 L container from each treatment set was "harvested" for sample water each sampling day.

The experiment matrix used for the MicroPat incubation duplicated the MesoPat experiment design (Table 1) and thereby consisted of 10 treatments. The experiment matrix for the three multistressor experiments (MultiPat, MultiArc and MultiMed outlined in Fig. S1 II) duplicated the corresponding mesocosm experiments at the same field sites (MesoPat, MesoArc and MesoMed), with one less C–glucose treatment and an additional pH manipulation (Table 1). The multistressor experiments thereby consisted of 16 treatments. pH manipulation was induced by adding a spike of HCl (trace metal grade) on day 0 only. For trace metal and H_2O_2 analysis, sample water from 20 L collapsible containers was extracted using a plastic syringe and silicon tubing which was mounted through the lid of each collapsible container.

Throughout, where changes in any incubation experiment are plotted against time, "day 0" is defined as the day the experimental gradient (zooplankton, DOC, pCO_2) was imposed. Time prior to day 0 was intentionally introduced during some experiments to allow water to equilibrate with ambient physical conditions after container filling. H_2O_2 concentration varies on diurnal timescales, and thus during each experiment where a time series of H_2O_2 concentration was measured sample collection and analysis occurred at the same time daily (± 0.5 h) and the order of sample collection was random. For the MesoMed time series, sampling occurred at 14:40 LT (local times) and for Gran Canaria at 11:00 LT. Sample times were selected to be intermediate with respect to the diurnal cycle (with peak H_2O_2 expected mid-afternoon, and the lowest H_2O_2 expected overnight).

2.3 Ancillary experiments

Four side experiments (1–4 below) were conducted to investigate potential links between bacterial–zooplankton abundance and extracellular H_2O_2 concentrations. Where specified, H_2O_2 concentrations were manipulated to form high-, medium- and low-H_2O_2 conditions by adding aliquots of either a 1 mM H_2O_2 solution (prepared weekly from H_2O_2 stock) to increase H_2O_2 concentration or bovine catalase (prepared immediately before use) to decrease H_2O_2 concentration. All treatments were triplicated. Catalase is photodeactivated and biological activity to remove extracellular H_2O_2 follows the diurnal cycle (Angel et al., 1999; Morris et al., 2016), so catalase and H_2O_2 additions were conducted at sunset in order to minimize the additions required. Bovine catalase was used as received (Sigma Aldrich) with stock solutions prepared from frozen enzyme (stored at -20 °C). Denatured catalase was prepared by heating enzyme solution to > 90 °C for 10 min.

(1) In Gran Canaria a 5 d experiment was conducted, using 5 L polypropylene bottles. After filling with offshore seawater, and the addition of macronutrients which matched the concentrations added to the Gran Canaria mesocosm (3.1 µM nitrate, 1.5 µM silicic acid and 0.2 µM phosphate), bottles were incubated under ambient light and temperature conditions within Taliarte Harbour. (2) In Crete, a similar 7 d incubation was conducted in the mesocosm pool facility us-

ing 20 L HDPE containers. Seawater was extracted from the baseline MesoMed mesocosm (no DOC or zooplankton addition) on day 11 and then incubated without further additions except for H_2O_2 manipulation. After day 5 no further H_2O_2 manipulations were made. (3) As per (2), seawater was withdrawn from the baseline MesoMed mesocosm on day 11 and then incubated without further addition except for H_2O_2 manipulation in 500 mL trace metal clean low-density polyethylene (LDPE) bottles under the artificial lighting conditions used for the MultiMed incubation. (4) A short-term (20 h) experiment was conducted in trace metal clean 4 L HDPE collapsible containers to investigate the immediate effect of grazing on H_2O_2 concentrations. Filtered (0.2 µm, Sartorius) coastal seawater (S 32.8, pH 7.9) water was stored in the dark for 3 d before use. The diatom *Skeletonema costatum* (NIVA-BAC 36 strain culture – CAA – from the Norsk institutt for vannforskning – NIVA) was used as a model phytoplankton grown in standard f/2 medium (Guillard and Ryther, 1962). Each treatment consisted of a total volume of 2 L seawater and contained macronutrients, 7.5 mL of the original medium (resulting in an initial chlorophyll *a* concentration of 3 µg L^{-1} in the incubations) and treated seawater containing the copepod *Calanus finmarchicus* corresponding to each desired density. The light regime was produced with fluorescent lighting with a mean luminous intensity of 80–90 µmol m^{-2} s^{-1}, and the temperature was maintained at 10.5–10.9 °C.

Light levels during all experiments (Table 1) were quantified using a planar Li-cor Q29891 sensor connected to a Li-cor Li-1400 data logger. Diurnal experiments measuring H_2O_2 concentrations in mesocosms or ambient surface (10 cm depth) seawater were conducted using a flow injection apparatus with a continuous flow of seawater into the instrument through a PTFE line as described previously (Hopwood et al., 2018). For extensive datasets, the diurnal range of H_2O_2 concentrations was determined as the difference between the means of the highest and lowest 10 % of data points.

2.4 Chemical analysis

2.4.1 H_2O_2

H_2O_2 samples were collected in opaque HDPE 125 mL bottles (Nalgene) which were pre-cleaned (1 d soak in detergent, 1 week soak in 1 M HCl, three rinses with de-ionized water) and dried under a laminar flow hood prior to use. Bottles were rinsed once with sample water, filled with no headspace and always analysed within 2 h of collection via flow injection analysis (FIA) using the Co(II) catalysed oxidation of luminol (Yuan and Shiller, 1999). FIA systems were assembled and operated exactly as per Hopwood et al. (2017), producing a detection limit of < 1 nM. Calibrations were run daily and with every new reagent batch using six standard additions of H_2O_2 (TraceSELECT, Fluka) within the range 10–300 nM to aged (stored at room temperature in the dark for > 48 h) seawater (unfiltered).

2.4.2 Macronutrients

Dissolved macronutrient concentrations (nitrate + nitrite, phosphate, silicic acid; filtered at 0.45 µm upon collection) were measured spectrophotometrically the same day as sample collection (Hansen and Koroleff, 2007). For experiments in Crete (MesoMed, MultiMed), phosphate concentrations were determined using the "MAGIC" method (Rimmelin and Moutin, 2005). The detection limits for macronutrients thereby inevitably varied slightly between the different mesocosm–microcosm–multistressor experiments (Table 1); however this does not adversely affect the discussion of results herein.

2.4.3 Carbonate chemistry

pH_T (except where stated otherwise, "pH" refers to the total pH scale reported at 25 °C) was measured during the Gran Canaria mesocosm using the spectrophotometric technique of Clayton and Byrne (1993) with *m*-cresol purple in an automated SensorLab SP101-SM system using a 25 °C thermostatted 1 cm flow cell exactly as per González-Dávila et al. (2016). pH during the MesoPat–MicroPat–MultiPat experiments was measured similarly as per Gran Canaria using *m*-cresol. During MesoArc–MultiArc–MesoMed–MultiMed experiments pH was measured spectrophotometrically as per Reggiani et al. (2016).

2.4.4 Biological parameters

Chlorophyll *a* was measured by fluorometry as per Welschmeyer (1994). Bacterial production was determined by incorporation of tritium-labelled leucine (^{3}H-Leu) using the centrifugation procedure of Smith and Azam (1992). Conversion of leucine to carbon (C) was done with the theoretical factor 3.1 kg C mol^{-1} leucine. In Gran Canaria, flow cytometry was conducted on 2 mL water samples which were fixed with 1 % paraformaldehyde (final concentration), flash frozen in liquid N_2 and stored at −80 °C until analysis. Samples were analysed (FACSCalibur, Becton Dickinson) with a 15 mW laser set to excite at 488 nm (Gasol and del Giorgio, 2000). Subsamples (400 µL) for the determination of heterotrophic bacteria were stained with the fluorochrome SYBR Green-I (4 µL) at room temperature for 20 min and run at a flow rate of 16 µL min^{-1}. Cells were enumerated in a bivariate plot of 90° light scatter and green fluorescence. Molecular Probes latex beads (1 µm) were used as internal standards. In Crete (MesoMed–MultiMed), the flow cytometry was conducted similarly except for the following minor changes: samples were fixed with 0.5 % glutaraldehyde (final concentration), yellow-green microspheres (1 and 10 µm diameter, respectively) were used as internal references during the analysis of bacterial and nanoflagellate populations,

and the flow rate was 79–82 µL min^{-1}. Subsamples (7–50 L) for zooplankton composition and abundance were preserved in 4 % borax buffered formaldehyde solution and analysed microscopically.

3 Results

3.1 H_2O_2 time series during outdoor mesocosm incubations; MesoMed and Gran Canaria

In order to understand the controls on H_2O_2 concentrations in incubations, time series of H_2O_2 are first presented for those experiments with the highest-resolution data. Also of interest are trends in bacterial productivity following the observation that H_2O_2 decay constants appear to correlate with bacterial abundance in a range of natural waters (Cooper et al., 1994). The concentration of H_2O_2 was followed in all treatments on all sampling days during the Gran Canaria and MesoMed mesocosms. In Gran Canaria, comparing mean (± SD) H_2O_2 in all mesocosms across a pCO_2 gradient (400–1450 µatm) with H_2O_2 in ambient seawater outside the mesocosms, H_2O_2 was generally elevated within the mesocosms compared to ambient seawater (ANOVA $p < 0.05$ for all treatments compared to ambient conditions). The mean and median ambient H_2O_2 concentrations throughout the experiment were at least 40 % lower than those in any mesocosm treatment (Fig. 1). This included the 400 µatm mesocosm which received no additions of any kind until the nutrient spike on day 18. The only exception was a short time period under post-bloom conditions when bacterial abundance peaked and daily integrated light intensity was relatively low (compared to the mean over the duration of the experiment) for 3 consecutive days (experiment days 25–27; Hopwood et al., 2018). No clear trend was observed with respect to the temporal trend in H_2O_2 and the pCO_2 gradient. H_2O_2 concentration in the baseline pCO_2 treatment was close to the mean (400–1450 µatm) for the duration of the 28 d experiment.

During MesoMed (Fig. 2) an additional mesocosm tank was filled (Tank 11) and maintained without any additions (no macronutrients, no DOC, no zooplankton) alongside the 10 mesocosm containers. As per the Gran Canaria mesocosm, H_2O_2 concentrations were also followed in ambient seawater throughout the duration of the MesoMed experiment. MesoMed was however conducted in an outdoor pool facility, so the ambient concentration of H_2O_2 in coastal seawater refers to a site approximately 500 m away from the incubation pool. Ambient H_2O_2 was generally higher than that observed within the mesocosm with a median concentration of 120 nM around midday (Fig. 2a).

H_2O_2 during the MesoMed experiment was relatively constant in terms of the range of concentrations measured over the 11 d duration of the experiment (Fig. 2), especially when compared to the Gran Canaria mesocosm (Fig. 1). A notable clustering of the high-zooplankton ("HG") and low-zooplankton ("LG") tanks was clearly observed between days 1 and 9 (Fig. 2) (addition of zooplankton took place immediately after day 1 sampling). H_2O_2 concentration in the high-zooplankton tanks initially declined more strongly than the low-zooplankton tanks and then rebounded together after day 5 (Fig. 2). Dilution experiments to estimate zooplankton grazing and zooplankton abundance (Fig. 2) both suggested that between days 3 and 7, the high- and low-grazing status of the mesocosms converged; i.e. grazing declined in the tanks to which zooplankton had initially been added and increased in the tanks to which no zooplankton had been added such that initial "high-grazing" and "low-grazing" labels became obsolete (Rundt, 2016). H_2O_2 concentration declined sharply in all treatments on day 11, except in the no-nutrient-addition mesocosm, coinciding with a pronounced increase in zooplankton abundance and occurring just after bacterial productivity peaked in all treatments (Fig. 2).

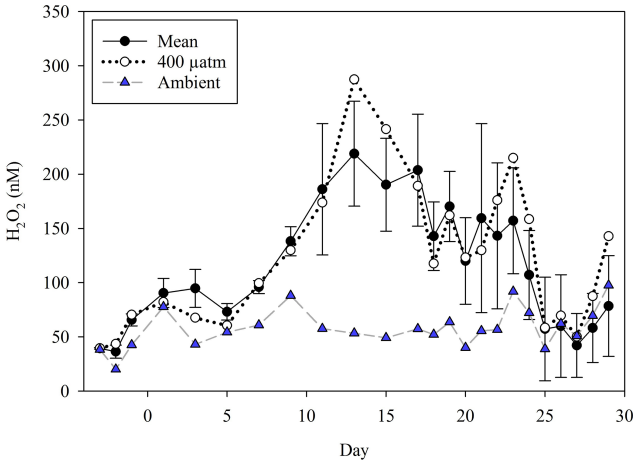

Figure 1. A summary of H_2O_2 over the duration of a pCO_2 gradient mesocosm in Gran Canaria. Data from Hopwood et al. (2018). The mean (± SD) H_2O_2 from all pCO_2 treatments is contrasted with the concentration in ambient surface seawater immediately outside the mesocosms. In addition to its inclusion in the mean, the baseline 400 µatm pCO_2 treatment is shown separately to allow comparison with ambient surface seawater.

H_2O_2 decay rate constants in the dark (measured using freshly collected seawater at the MesoMed field site over 24 h and assumed to be first order) were 0.049 h^{-1} (unfiltered) and 0.036 h^{-1} (filtered, Sartorius 0.2 µm) corresponding to half-lives of 14 and 19 h, respectively, which are within the range expected for coastal seawater (Petasne and Zika, 1997).

3.2 H_2O_2 trends during 20 L scale indoor MultiPat, MultiMed and MicroPat incubations

A sustained decline in H_2O_2 concentration was found whenever ambient seawater was moved into controlled temperature rooms with artificial diel light cycles (e.g. Fig. 3), which

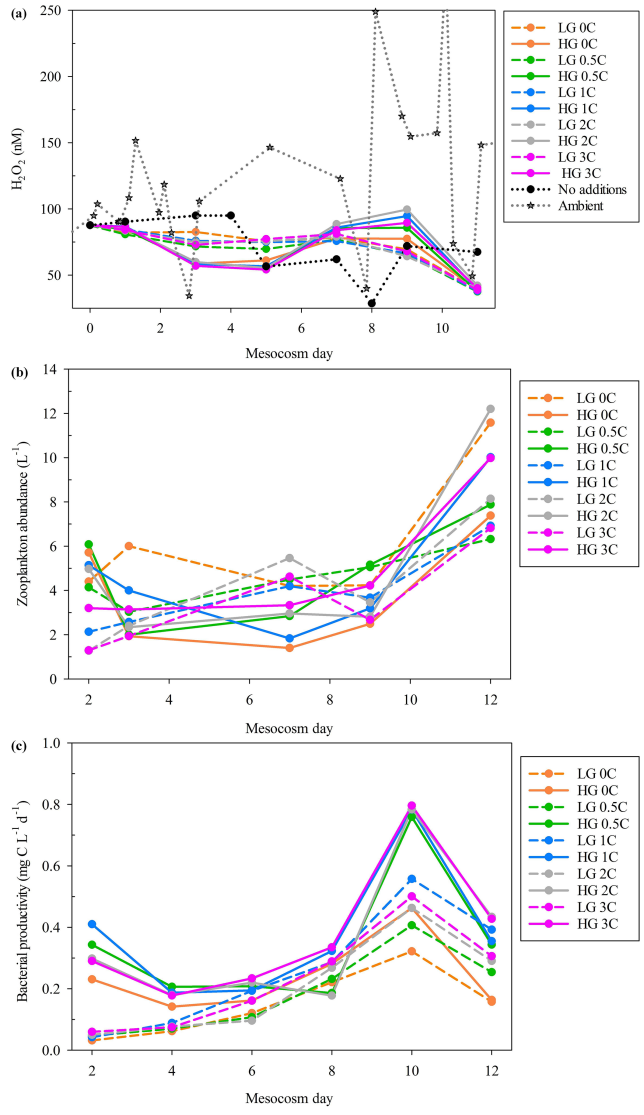

Figure 2. **(a)** H_2O_2 in all mesocosms during MesoMed in Gouves, Crete. A 10-treatment matrix (as per Fig. S1) was used. **(b)** Zooplankton abundances showed a rapid convergence in the HG–LG (high-grazing, low-grazing) status of the mesocosms after day 2. **(c)** The trend in bacterial productivity showed broad similarity within the HG and LG treatment groups.

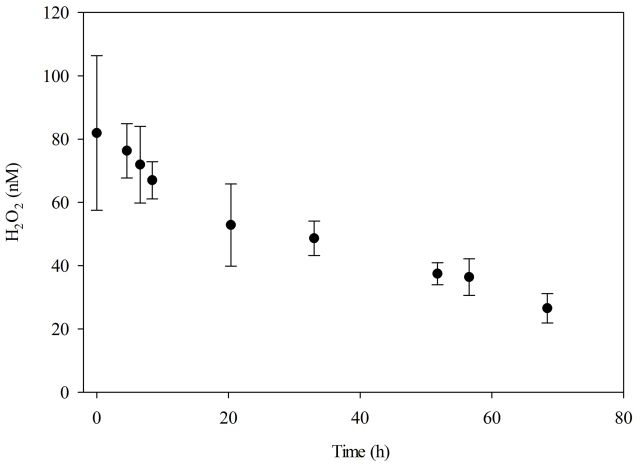

Figure 3. Seawater from MesoMed (without macronutrient, DOC or zooplankton amendment) was used to fill a 20 L HDPE container, which was then incubated under the synthetic lighting used in the MultiMed experiment for 72 h with regular subsampling for analysis of H_2O_2 ($\pm$ SD).

were used to incubate all 20 L scale multistressor and microcosm experiments discussed herein (Table 1). Final H_2O_2 concentrations in these 20 L scale experiments were thereby generally low compared to those measured in corresponding ambient surface waters and to the corresponding outdoor experiments in the same locations with natural lighting.

H_2O_2 concentrations by the end of the MultiMed experiments (day 9) were universally low compared to the range found in comparable ambient waters and the outdoor mesocosm incubation conducted at the same field site (Fig. 2). As was the case in the MesoMed experiment, a clear difference was noted between H_2O_2 concentrations in the high- and low-zooplankton-addition treatments (Fig. 4b), with the high grazing always resulting in higher H_2O_2 concentrations (t test, $p < 0.001$). Any effect of pH was less obvious, with similar results obtained between ambient-pH (initially 8.08 ± 0.02) and low-pH (initially 7.64 ± 0.02) treatments (Fig. 4a), and thus low- and ambient-pH treatments are not distinguished in Fig. 4b and c. An effect of the imposed C gradient on H_2O_2 concentrations was notable in both the high- and low-grazing treatments, yet the effect operated in the opposite direction (Fig. 4b). In high-grazing treatments, increasing C corresponded to increasing extracellular H_2O_2 concentrations (linear regression coefficient 4.5 ± 2.3); whereas in low-grazing treatments, increasing C corresponded to decreasing extracellular H_2O_2 concentrations (linear regression coefficient -6.3 ± 0.97). Bacterial productivity increased with added C in both high-grazing (linear regression coefficient 0.31 ± 0.1) and low-grazing treatments (linear regression coefficient 1.2 ± 0.1), but there was a more pronounced increase under low-grazing conditions (Fig. 4c).

At the end of the MultiPat experiment (day 8), H_2O_2 concentrations were similarly low compared to ambient surface waters at the Patagonia field site (Fig. 5a), although there was a greater range of results. In the low-pH treatment (initially 7.54 ± 0.09), H_2O_2 concentrations were significantly higher (Mann–Whitney rank sum test $p = 0.02$) compared to the unmodified pH treatment (initially 8.01 ± 0.02). However, two of the low-pH treatments with particularly high H_2O_2 were outliers (defined as 1.5 IQR) when considering the data as consisting of two pH groups. Without these two data points, there would be no significant difference between H_2O_2 in high and low treatments ($p = 0.39$). Contrary to the results from the MultiMed experiment (Fig. 4), there was no

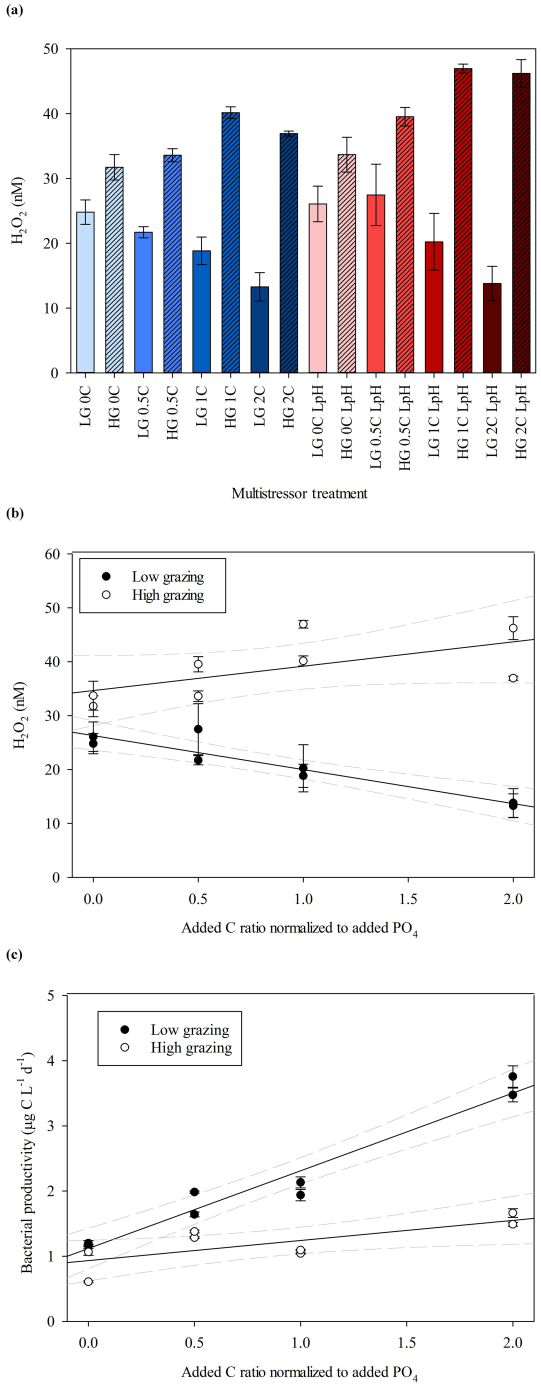

Figure 4. (a) H_2O_2 concentrations at the end of the MultiMed experiment (day 9). Ambient pH (blue), low pH (red); high grazing (hashed); carbon (C) added at 0, 0.5, 1.0, 1.5 and 2.0 times the Redfield carbon: phosphate ratio. **(b)** Plotting both ambient- and low-pH data points together, which exhibited no statistically significant difference in H_2O_2 concentrations, final H_2O_2 concentration showed contrasting trends between high- and low-grazing treatments over the added C gradient. The 95 % confidence intervals are shown. **(c)** Bacterial productivity, measured via leucine incorporation, during the same experiments. Error bars show ± SD of at least triplicate measurements.

significant difference between high- and low-grazing treatments (Mann–Whitney rank sum test $p = 0.65$). Bacterial productivity also showed similar results between the high- and low-grazing treatments (Fig. 5b). Data from day 5 (the last day bacterial productivity was measured) showed a similar gradient in increased bacterial productivity with added C for both high- and low-grazing treatment groups (linear regressions HG 0.64, R^2 0.70 and LG 0.72, R^2 0.92).

The MicroPat experiment, also conducted using 20 L HDPE containers and artificial lighting, yielded no clear trend with respect to H_2O_2 concentrations over the imposed C gradient (Fig. 6, day 11), but the high-grazing treatments were associated with higher H_2O_2 concentrations (t test, $p = 0.017$). Bacterial productivity was not systematically different across the high- and low-grazing treatment groups, nor was there as clear a trend in bacterial productivity with respect to the added C gradient (Fig. 6c) compared to the MultiPat (Fig. 5b) or MultiMed (Fig. 4c) experiments. Error bars show ± SD of at least triplicate measurements.

3.3 Diurnal cycling of H_2O_2; results from the Mediterranean

In addition to the trends observed over the duration of multi-day incubation experiments, a diurnal variability in H_2O_2 concentrations is expected. The diurnal cycle of H_2O_2 concentrations during MesoMed was followed in the no-addition tank (number 11) over 2 d with markedly different H_2O_2 concentrations (Fig. 7). An additional cycle was monitored at a nearby coastal pier (Gouves) for comparative purposes. The mean difference between mid-afternoon and early-morning H_2O_2 could also be deduced from discrete time points collected over the experimental duration in seawater close to the pool facility. All time series are plotted against local time (UTC+1). Sunrise–sunset was as follows: (15 May) 06 : 15, 20 : 17; (19 May) 06 : 12, 20 : 20. All three time series showed the expected peak in H_2O_2 concentrations during daylight hours, but the timing of peak H_2O_2 concentration and the range of concentrations observed differed between mesocosms and coastal seawater. The intraday range in H_2O_2 concentrations in Gouves, and the afternoon peak in H_2O_2, (Fig. 7) was similar to that observed previously in Gran Canaria (Hopwood et al., 2018). Yet both the mesocosm diurnal time series exhibited notably limited diurnal ranges, and peak H_2O_2 concentration occurred earlier, around midday (Fig. 7), than in coastal waters.

3.4 Ancillary experiments to investigate links between microbial groups (bacterial, zooplankton) and extracellular H_2O_2

In addition to comparing H_2O_2 concentrations in different incubation experiments to assess the effect of experiment set-up on extracellular H_2O_2 concentrations, potential links between microbial groups and H_2O_2 were ex-

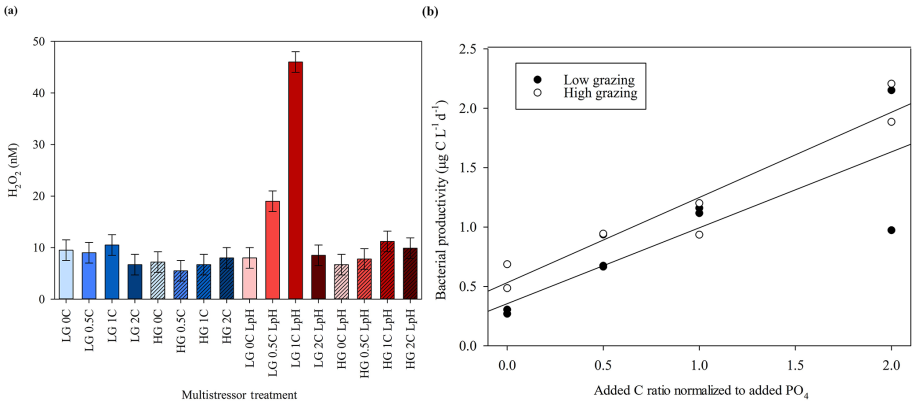

Figure 5. (a) H_2O_2 concentrations at the end of the MultiPat experiment. Normal pH (blue); low pH (red); high grazing (hashed); DOC added at 0, 0.5, 1.0, and 2.0 times the Redfield carbon (C) : phosphate ratio indicated by increasing colour density. **(b)** Plotting both high- and low-pH data points together (which exhibited no statistically significant difference in H_2O_2 concentrations), bacterial productivity showed similar trends between the HG and LG treatments.

plored. The MesoPat–MesoArc–MesoMed, MicroPat and MultiPat–MultiArc–MultiMed experiments all included a high- and low-zooplankton addition treatment (Table 1). Over a 20 h incubation (4 h darkness, 16 h light) in an experiment with varying concentrations of copepods (0–10 L^{-1}) grazing on an intermediate density of a diatom (initially 3 µg L^{-1} chlorophyll *a*), H_2O_2 concentrations showed no inter-treatment differences (Fig. 8). A diatom was selected as phytoplankton stock because cell normalized H_2O_2 production rates for diatoms appear to be generally at the low end of the observed range for phytoplankton groups (Schneider et al., 2016). Fe(II) concentration (measured at the same time as per Hopwood et al., 2020) also appeared to be unaffected by the copepod density as the difference between treatments was almost negligible (< 0.04 nM).

At the end of the MesoMed experiment, seawater (extracted from the baseline treatment from the mesocosm on day 11) was used in two side experiments. During both the extracellular H_2O_2 concentration was manipulated, with each treatment triplicated. In all cases the mean ($\pm$ SD) of three replicate treatments is reported. The high–medium–low H_2O_2 concentration gradient used in each experiment was determined by considering the ambient concentration of H_2O_2 in the mesocosms (e.g. Fig. 2) and in ambient seawater close to the mesocosm facility. After the first daily H_2O_2 measurements were made, the required spikes to maintain the desired H_2O_2 gradient were calculated based on measured rates of H_2O_2 decay. H_2O_2 and catalase spikes were then added at sunset followed by gentle mixing.

A test specifically to investigate the effect of the multistressor–microcosm experimental set-up on bacterial activity was conducted in 500 mL trace metal clean LDPE bottles under the artificial lighting conditions ($\sim$ 80 µmol m^{-2} s^{-1}) used for the MultiMed experiment. H_2O_2 concentrations again verified that manipulation with H_2O_2 spikes successfully created a low-, medium- and high-H_2O_2 treatment (mean for triplicate low, medium and high treatments: 40 ± 2, 120 ± 6, 230 ± 7 nM H_2O_2). Bacterial production showed no statistically significant (ANOVA, $p = 0.562$) difference between triplicate low- (1.69 ± 0.28 µg C L^{-1} d^{-1}), medium- (1.30 ± 0.60 µg C L^{-1} d^{-1}) and high- (1.29 ± 0.56 µg C L^{-1} d^{-1}) H_2O_2 treatments.

For a concurrent manipulation in the Mediterranean using 20 L HDPE containers incubated outdoors, a gradient in H_2O_2 concentrations was similarly imposed. These manipulations successfully produced a clear gradient of H_2O_2 conditions with relatively consistent H_2O_2 concentrations within each triplicated set (Fig. 9a). After day 5 no further manipulations were conducted and H_2O_2 accordingly began to converge towards the medium (no H_2O_2 spike, no active catalase spike) treatment. Flow cytometry, conducted on low, medium and high samples at 8×24 h intervals over the experiment duration, measured no significant (ANOVA, $p > 0.05$) difference between the three treatments for cell counts of any group (bacteria are shown as an example, Fig. 9c).

A similar side experiment was conducted in Gran Canaria, but one critical difference was the addition of macronutrients at the start of the experiment, as per the mesocosm at the same location (Table 1). Measurement of H_2O_2 concentrations, which were initially 43 ± 1 nM (mean of all 3×3 replicates at day 0), confirmed that a gradient was maintained over the 5 d duration of the experiment (mean 210 ± 113, 62 ± 14 and 47 ± 8 nM in the high-, medium- and low-H_2O_2 treatments, respectively). Some modest shifts in phytoplankton group abundance were observed over the duration of this experiment. Slightly higher cell counts of bacteria were consistently observed in the low-H_2O_2 treatment relative to the medium- and high-H_2O_2 treatments (Fig. 9d). Only the difference between the low and medium–high treatments was significant (ANOVA, $p = 0.028$) – no significant difference was found between the medium- and high-H_2O_2 treatments (ANOVA, $p = 0.81$).

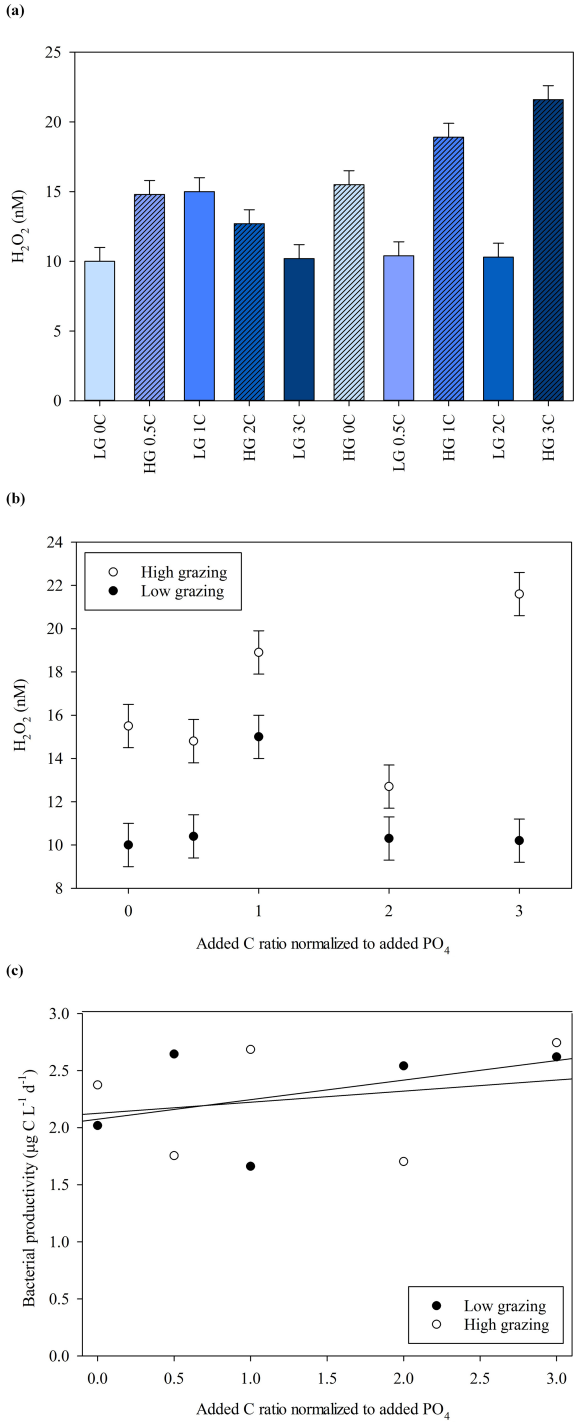

Figure 6. **(a)** H_2O_2 concentrations at the end of the MicroPat experiment. High-grazing treatments are hashed; DOC added at 0, 0.5, 1.0, 2.0 and 3.0 times the Redfield carbon (C) : phosphate ratio indicated by increasing colour density. **(b)** No clear trend was evident across the DOC gradient, but high grazing was consistently associated with higher H_2O_2 concentration. **(c)** Bacterial productivity in the same experiment. Error bars show ± SD of at least triplicate measurements.

4 Discussion

4.1 Bacteria, zooplankton and extracellular H_2O_2 trends

During all meso–multi–micro experiments and the Gran Canaria mesocosm (Table 1), data were available on the abundance of bacteria and zooplankton throughout the experiment. We focus on zooplankton because of the top-down control they may exert on primary production and the potential for grazing to release trace species into solution which may affect H_2O_2 biogeochemistry. Bacteria were a key focus because of the hypothesis that bacteria are, via the production of peroxidase–catalase enzymes, the main sink for H_2O_2 in surface aquatic environments (Cooper et al., 1994).

Throughout, no clear effect of changing pH on H_2O_2 concentrations was evident. The 440–1450 µatm pCO_2 gradient applied in Gran Canaria, which corresponded to a pH range of approximately 7.5–8.1, and the contrasting ambient–low pH (a reduction in pH of 0.4–0.5 from ambient waters was imposed) applied during three multistressor incubations (Table 1) exhibited no obvious change in equilibrium extracellular H_2O_2 concentration. Similarly no change was evident in Gran Canaria when contrasting the diurnal cycling of H_2O_2 in the 400 and 1450 µatm pCO_2 treatments (Hopwood et al., 2018). In the incubation experiments, whenever there was a sustained difference in extracellular H_2O_2 concentrations between treatment groups (MesoMed, Fig. 2; MultiMed, Fig. 4), the main difference arose between high- and low-zooplankton addition treatments. However, determining the underlying reason for this was complicated by the shifts in zooplankton abundance during the experiments (e.g. Fig. 2b).

The MultiPat (Fig. 5) and MicroPat (Fig. 6) incubations showed no significant effect of increased zooplankton abundance on extracellular H_2O_2. Two reasons for this can be considered. First, in Patagonia the initial ratio of zooplankton between the high and low treatments was the smallest of the experiments herein (17 : 14), and thus a large difference might not have been anticipated compared to the experiments where this initial ratio was always considerably higher. However, the mean ratio of HG : LG zooplankton by the end of MultiPat had increased to 9 : 5. By comparison, during MesoMed (when the HG : LG zooplankton abundance converged during the experiment, Fig. 2b) the HG : LG ratio after day 1 varied within the range 0.32–1.6 and thus the final ratio of 1.8 in MultiPat was not particularly low. A more distinct difference however arose in bacterial productivity (Fig. 5b). Unlike MesoMed, MultiPat and MicroPat showed little difference in bacterial productivity between the high- and low-grazing treatments. Thus the effects of zooplankton with respect to shifts in the abundance of other microbial groups (rather than grazing itself) may be the underlying reason why extracellular H_2O_2 concentrations sometimes, but not consistently, changed between high- and low-grazing treatments.

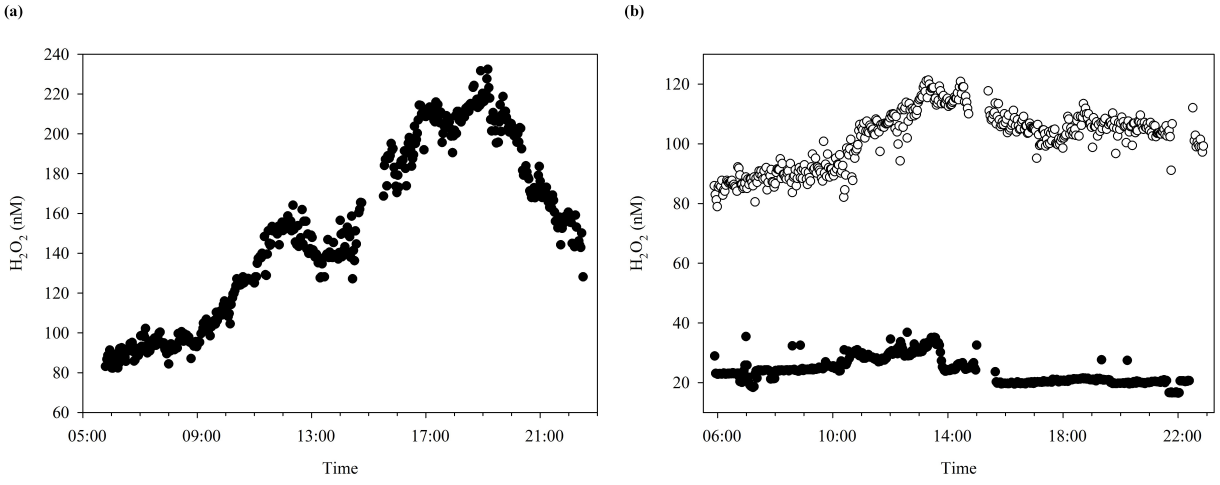

Figure 7. (a) Diurnal cycling of H_2O_2 in coastal seawater (Gouves, Crete 17 May) and **(b)** in the no addition tank (number 11) during the MesoMed mesocosm on 15 May (open circles) and 19 May (closed circles) 2016 (experiment days 4 and 8, respectively).

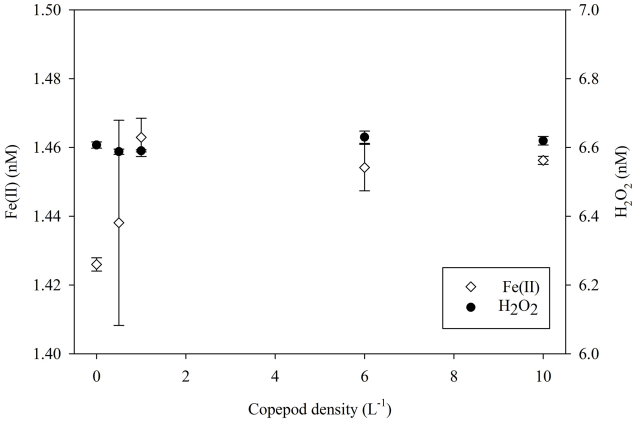

Figure 8. H_2O_2 and Fe(II) concentrations in a culture of diatoms growing in coastal seawater after 20 h of incubation with a zooplankton gradient imposed by addition of copepods. Error bars show ± SD of triplicate measurements.

Second, in any case H_2O_2 concentrations at the end of the Patagonian experiments (MesoPat, MicroPat and MultiPat) were also very low (almost universally < 20 nM), and thus the signal : noise ratio was unfavourable for detecting differences between treatments.

Furthermore, the effect of higher zooplankton populations was not a consistent positive or negative change in extracellular H_2O_2. During the post-nutrient addition phase in Gran Canaria, the single treatment with slower nutrient drawdown (mesocosm 7) due to high grazing pressure exhibited relatively high H_2O_2 (Hopwood et al., 2018). During MesoMed, increases in zooplankton abundance coincided with decreases in H_2O_2 concentration (Fig. 2). Similarly, during MultiMed (Fig. 4), the effect of adding zooplankton was the same; high-zooplankton treatments exhibited low H_2O_2 concentration. As high zooplankton levels are correlated during some experiments, and anti-correlated in others, with H_2O_2, the underlying cause did not appear to be that H_2O_2 is generally produced by the process of grazing (i.e. as a by-product of feeding). Further support for this argument was found in the results of a simple side experiment adding copepods (*Calanus finmarchicus*) to a diatom culture (*Skeletonema costatum*) (Fig. 8). No measurable change in extracellular H_2O_2 concentration was found at higher densities of copepods either during a 16 h light incubation or after 4 h of incubation in the dark (Fig. 8). There are two obvious limitations in this experiment; a different result may have been obtained with a different combination of copepod and phytoplankton, and standard f/2 medium contains the ligand ethylenediaminetetraacetic acid (EDTA) which may affect H_2O_2 formation rates by complexing trace species involved in H_2O_2 cycling (e.g. dissolved Fe and Cu). Nonetheless, it is known that cellular ROS production rates vary at the species level (Schneider et al., 2016; Cho et al., 2017), so shifts in species composition as a result of zooplankton addition are a plausible underlying cause of changes in extracellular H_2O_2 concentration. We summarize that any correlation between H_2O_2 and zooplankton thereby appears to have arisen from the resulting change in the abundance of microbial species and thus the net contribution of biota to extracellular H_2O_2 concentration, rather than from the act of grazing itself.

Bacteria are expected to be a dominant H_2O_2 sink in most aquatic environments (Cooper et al., 1994). Here the correlation between extracellular H_2O_2 and bacteria cell counts was much stronger in some experiments than others (R^2 from 0.09 to 0.55). A key reason for this may simply be the generally low H_2O_2 concentrations measured in most of our experiments. At the low H_2O_2 concentrations of < 50 nM observed during most experiments, the influence of any parameter on H_2O_2 removal would be more challeng-

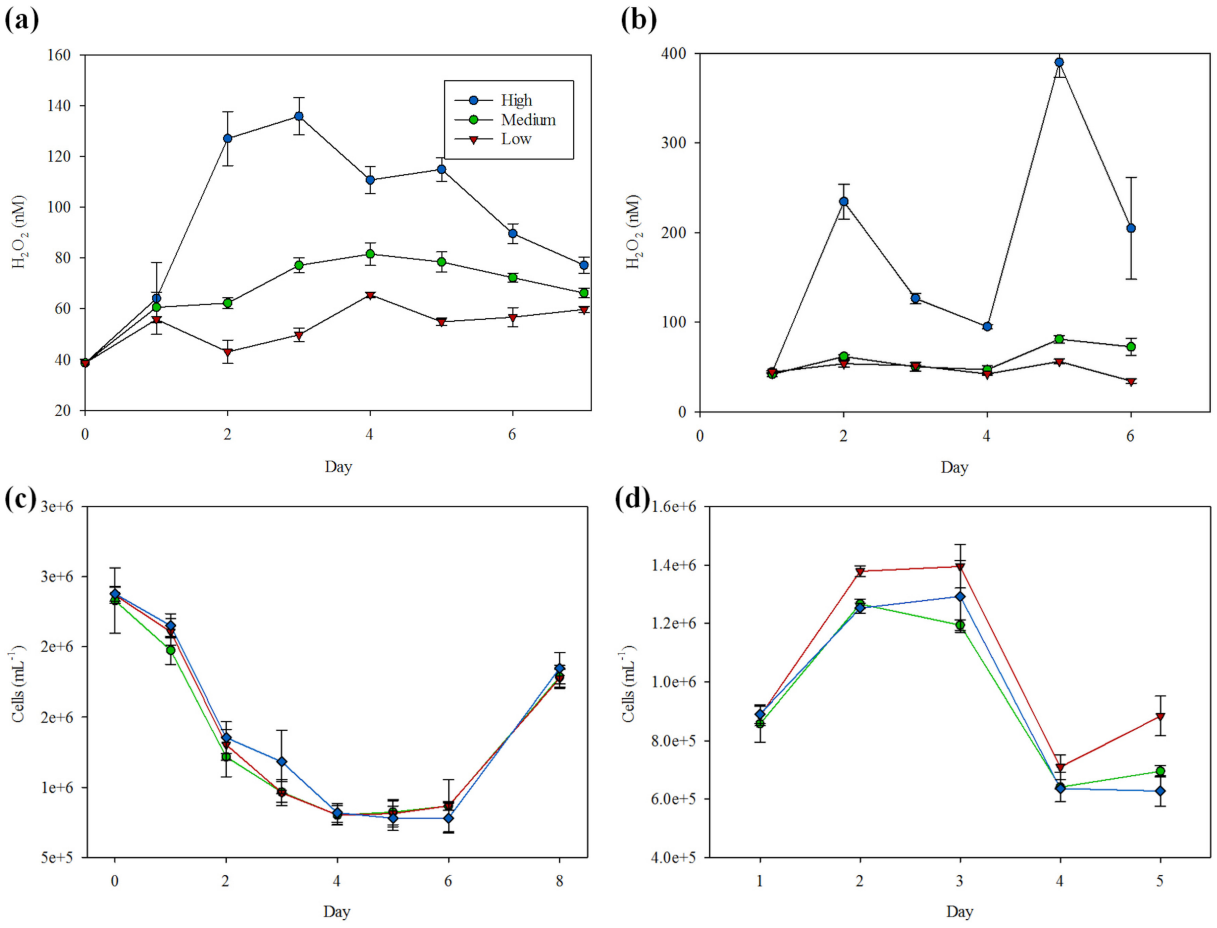

Figure 9. **(a)** H_2O_2 gradient during the 20 L scale Mediterranean side experiment where H_2O_2 gradient was created with H_2O_2 spikes and catalase. **(b)** H_2O_2 gradient during the 20 L scale Gran Canaria side experiment where a H_2O_2 gradient was created with H_2O_2 spikes. **(c)** Bacteria abundance during the Mediterranean experiment. **(d)** Bacteria abundance for the Gran Canaria experiment. Mean and standard deviations of triplicate treatments are plotted in all cases.

ing to determine from an analytical perspective due to reduced signal : noise ratio. However, the H_2O_2 defence mechanism of organisms may also be sensitive to ambient H_2O_2 concentrations. Morris et al. (2016) suggest that microbial communities exposed to high H_2O_2 have elevated H_2O_2 defences. If the microbial communities here exhibited a dynamic response to H_2O_2 concentrations in terms of their extracellular H_2O_2 removal rates, this would dampen the correlation between bacterial abundance and H_2O_2 concentrations. Combing all available H_2O_2 concentrations for which the corresponding total bacterial cell counts are available (Fig. 10) from all experiments (except the side experiments where H_2O_2 was manipulated using catalase or H_2O_2 spikes) provides some limited evidence for the dominance of bacteria as a H_2O_2 sink. There was a notable absence of high-H_2O_2, high-bacteria data points in any experiment (Fig. 10). The observed distribution is therefore consistent with a scenario where bacteria dominate H_2O_2 removal, but other factors (possibly including experiment design; see Sect. 4.2) can also lead to low-H_2O_2 conditions independently of bacterial abundance.

4.2 Changes in extracellular H_2O_2 due to experiment design

When all available H_2O_2 data points were normalized to ambient H_2O_2 at the respective field site, which varied between our locations (Table 2), some qualitative inter-experiment trends were evident. Experiments incubated with artificial lighting (MultiPat–MultiArc–MultiMed and MicroPat) generally exhibited the lowest concentrations, while higher normalized H_2O_2 concentrations were observed in the closed HDPE mesocosms (MesoMed, MesoPat, MesoArc) and then the open Gran Canaria mesocosm experiment (Fig. 11b and c). This is not surprising considering the light arrangements for these experiments (Table 1). The Gran Canaria experiment was practically unshaded with surface seawater exposed to natural sunlight. The closed HDPE mesocosms (MesoMed, MesoPat, MesoArc) experienced natural

Table 2. Range of water properties in freshly collected coastal seawater at each site where the mesocosms were conducted. "n/a" denotes "not applicable". [a] Temperature of pool facility at HCMR. [b] Coastal seawater approximately 500 m from HCMR facility.

Location	Season	Latitude	Salinity	Temperature (°C)	H_2O_2 (nM)
Taliarte, Gran Canaria	March 2016	30.0° N	36.6–36.8	18–19	10–50
Gouves, Crete	May 2016	35.3° N	n/a	19–20[a]	34–410[b]
Comau fjord, Patagonia	November 2014	42.4° S	3.9–12.8	9.7–13	120–680
Kongsfjorden, Svalbard	July 2015	78.9° N	9.0–35.2	5.0–9.0	10–100

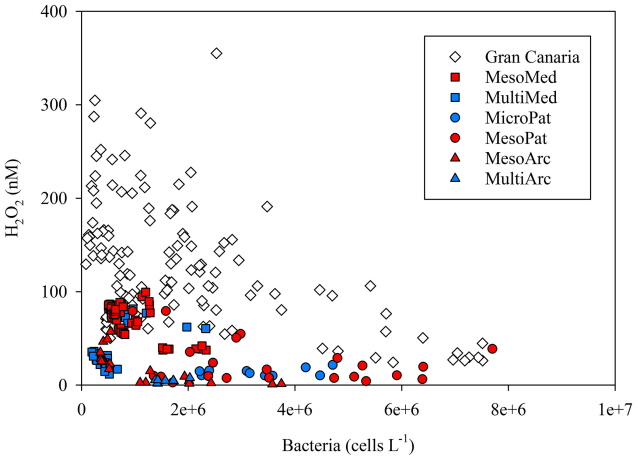

Figure 10. Bacterial cell counts and H_2O_2 for all available data from all incubation experiment time points where both measurements were made within 24 h of each other.

sunlight but after attenuation through 1–2 cm of HDPE plastic. Whilst the transmission of different light wavelengths through these HDPE containers was not tested during our experiments, 1–2 cm of polyethylene should strongly attenuate the UV component of sunlight. The 20 L scale experiments (MultiMed, MultiPat, MultiArc and MicroPat) were conducted using identical synthetic lighting with lamps selected to as closely as possible replicate the wavelength distribution of natural sunlight. However, the fluorescent light distribution is still deficient, relative to sunlight, in wavelengths < 400 nm, which is the main fraction of light that drives H_2O_2 formation in surface seawater (Kieber et al., 2014), and these containers still mitigated the limited UV exposure with a 1 mm HDPE layer which would further reduce the UV component of incoming light.

During all periods when high-resolution H_2O_2 time series were obtained, a clear diurnal trend was observed with a peak in H_2O_2 concentration occurring around midday (Fig. 7). Yet the range of concentrations within the two MesoMed diurnal experiments (31.2 ± 2.3 and 14.5 ± 2.7 nM) was limited compared to those observed previously within a Gran Canaria mesocosm (96 ± 4 and 103 ± 8 nM; Hopwood et al., 2018). For comparison, the diurnal ranges reported in further offshore surface waters of the Atlantic, Gulf of Mexico and sub-tropical equatorial Pacific along the Peruvian shelf are 20–30 nM (Yuan and Shiller, 2001), 40–70 nM (Zika et al., 1985) and 40 nM[1], respectively, with no clear systematic trend associated with changes in mixed-layer depth (Fig. 11a). Within mesocosms and the coastal mesocosm field sites, the range was more variable. Notably, the MesoMed diurnal ranges (15 and 31 nM) were considerably lower than those observed at two corresponding coastal sites (one monitored over a single diurnal cycle, 127 ± 5 nM; one at regular intervals over the duration of the experiment, 118 ± 94 nM). Conversely, for the Gran Canaria mesocosm the ∼ 100 nM diurnal range was much greater than that observed (27.0 ± 3.1 nM) in ambient surface waters (Fig. 11a).

There are inevitably limits to what can be determined from contrasting available data on H_2O_2 concentration from multiple incubation experiments due to the different experiment designs (see Table 1). Yet the experiment set-up with respect to moderating light during an experiment appears to be critical to establishing the equilibrium H_2O_2 concentration and can either enhance or retard the extracellular concentration of H_2O_2 during the experiment. The diurnal range plotted for all mesocosm experiments reflected increased H_2O_2 concentrations during daylight hours. This concentration range was suppressed in the closed HDPE containers (e.g. MesoMed), yet enhanced in open polyurethane bags (Gran Canaria). During the multistressor and microcosm experiments, incubated indoors in 20 L HDPE containers, the diurnal range in H_2O_2 concentrations was suppressed sufficiently that no increase in H_2O_2 was apparent during simulated daylight hours. Lighting conditions for the experiments therefore could explain both the contrasting change in the diurnal range of H_2O_2 (Fig. 11a) and the shift in the gradient between bacteria and H_2O_2 under different experiment conditions (Fig. 10).

4.3 ROS, bacteria and the Black Queen Hypothesis

Results from experiments where H_2O_2 concentrations were manipulated were mixed. In a side experiment after MesoMed, there was no evidence of strong positive or negative effects of H_2O_2 concentrations on any specific microbial group (Fig. 9). In Gran Canaria, under different experi-

[1] Unpublished data kindly provided by Insa Rapp (GEOMAR).

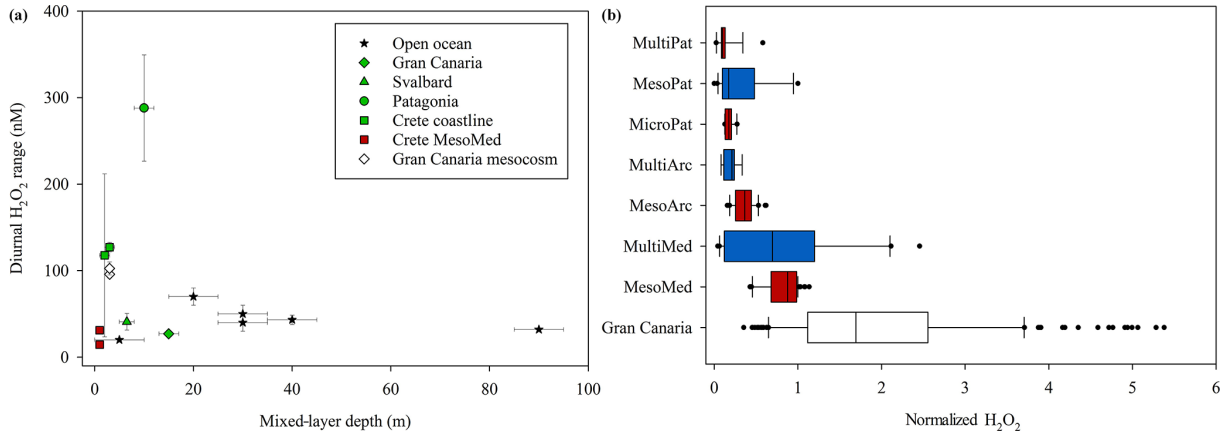

Figure 11. (a) Observed diurnal ranges in H_2O_2 concentrations. Black stars show literature surface marine values and green shapes in situ experiments corresponding to experiment field site locations. **(b)** H_2O_2 across all experiments as a fraction of ambient H_2O_2. For the Meso–Multi field sites (Mediterranean, Arctic and Patagonia) red bars are outdoor mesocosms and blue shapes indoor incubations. The median; 10th, 25th, 75th, and 90th percentiles; and all outliers are shown.

mental conditions (macronutrients were added, whereas for the MesoMed side experiment no macronutrient spike was added), a small increase in bacterial abundance was found at low H_2O_2 concentrations (+27 %, Fig. 9d). This result alone should be interpreted with caution, as the addition of catalase can have other effects in addition to lowering H_2O_2 concentration (Morris, 2011), yet it is intriguing to consider the role of H_2O_2 as an intermediate in the cycling of DOM alongside the role of bacteria as the dominant H_2O_2 sink.

Photochemistry both enhances the lability of DOM (Bertilsson and Tranvik, 1998; Keiber et al., 1990) (thus making it more bioavailable as a substrate for bacteria) and causes the direct photochemical oxidation of DOM into dissolved inorganic carbon (Miller and Zepp, 1995; Granéli et al., 1996) (thus rendering it unavailable as a substrate for bacteria). ROS may enhance both of these processes, but few attempts have been made to determine the effect of manipulating ROS concentrations on photochemical DOM degradation rates, especially in the marine environment and at nanomolar concentrations (Pullin et al., 2004). Yet in experiments using furfuryl alcohol to suppress ROS in lake water, the rate of dissolved inorganic carbon formation when exposed to light decreased 20 % and bacterial populations when later incubated in this ROS-quenched water were 4-fold higher than water with "normal" ROS activity (Scully et al., 2003) implying that ROS removal was beneficial for bacteria. The results of experiments conducted in freshwater environments are not directly applicable to the marine environment, due to the different conditions in the ambient water column, but it is plausible that a similar mechanism underpinned the increase in bacteria abundance observed in Gran Canaria following the artificial lowering of H_2O_2 concentrations (Fig. 9). A large difference in bacterial populations between the presence and absence of some ROS species (Scully et al., 2003) raises interest in how important an influence changes in ROS concentration could be on the availability of DOM for bacterial productivity in the surface marine environment when more subtle changes are made to ambient H_2O_2 concentrations. If heterotrophic bacteria are the dominant H_2O_2 sink (Cooper et al., 1994), which the observed trend between bacterial abundance and extracellular H_2O_2 across a broad range of incubation experiments is consistent with (Fig. 10), this is also interesting in light of the Black Queen Hypothesis. The BQH (Morris et al., 2012) assumes that the sole major benefit of producing enzymes that remove extracellular H_2O_2 is protection against the oxidative stress associated with high H_2O_2 concentrations – which is a communal benefit (Zinser, 2018). Yet, if increasing extracellular H_2O_2 concentrations accelerate the degradation of labile DOM to dissolved inorganic carbon, a second benefit of H_2O_2 removal in productive waters is the enhanced availability of this DOM to heterotrophs. Thus, under some circumstances, it could possibly be more favourable for heterotrophic species to maintain genes associated with the removal of H_2O_2 than autotrophic species because, in addition to the shared communal benefit of lowering oxidative stress, heterotrophs would suppositionally benefit more directly than autotrophs from the enhanced stability of labile DOM under low-H_2O_2 conditions. However, whilst H_2O_2 is a reactive species, at the concentrations present in the marine environment the direct effects of changing H_2O_2 concentration on the abundances of different microbial groups (e.g. Fig. 9) are clearly minor. A specific challenge with determining the effect(s) of H_2O_2 concentration on any biogeochemical processes, and vice versa, is that the diurnal variability in H_2O_2 concentration is always large compared to inter-treatment differences in H_2O_2 concentration within individual experiments (e.g. Fig. 11). High-resolution data are therefore clearly required to properly interpret H_2O_2–microbe interactions and to better quantify the

subtle links between H_2O_2 cycling and microbial functioning.

5 Conclusions

Extracellular H_2O_2 concentrations and bacterial abundances over a broad range of incubation experiments conducted in the marine environment support the hypothesis that bacterially produced enzymes are the dominant H_2O_2 sink. If heterotrophic bacteria are generally the main sink for H_2O_2 in surface marine environments, it is of interest to determine whether changes in extracellular H_2O_2 concentration measurably affect the photochemical transformation of DOM transformation to dissolved inorganic carbon. If increasing equilibrium ROS concentrations decreases the availability of labile DOM as a substrate for heterotrophs, this may affect which group or species produce catalase–peroxidase enzymes in productive waters.

It was apparent from comparing multiple experiments that incubation experiment design is also a strong influence on H_2O_2 concentrations. Closed HDPE mesocosms exhibited concentrations 10 %–90 % lower than those expected in the corresponding ambient seawater, whereas an open (lidless) mesocosm exhibited concentrations 2–6-fold higher than ambient seawater. The diurnal range in H_2O_2 within incubations was also correspondingly increased in experiments where H_2O_2 concentration was artificially high, and vice versa where H_2O_2 concentration was artificially low, suggesting enhanced, or reduced, photochemical stress over the diurnal cycle. Incubated experiments thus poorly mimic the biogeochemistry of reactive photochemically formed trace species.

Data availability. Data from Gran Canaria are appended to Hopwood et al. (2018). Full datasets for the remaining mesocosm and microcosm experiments are available from: https://doi.pangaea.de/10.1594/PANGAEA.911130 (Sanchez et al., 2020).

Supplement. The supplement related to this article is available online at: https://doi.org/10.5194/bg-17-1309-2020-supplement.

Author contributions. MJH, DP, JAGU, EPA, DT and MA designed the study. MJH, NS, DP, ØL, JAGU, MVA, JA, SB, YH, IK, TTK and TMT undertook work at one or more of the mesocosm–microcosm–multistressor experiments. MJH, NS, DP, ØL, JAGU, JA, LB, SB, YH, TTK, IS and TMT conducted analytical work. MJH, NS, DP, SB and TMT interpreted the data. MJH coordinated the writing of the manuscript with input from other authors.

Competing interests. The authors declare that they have no conflict of interest.

Acknowledgements. The Ocean Certain and KOSMOS/PLOCAN teams assisting with all aspects of experiment logistics and organization are thanked sincerely for their efforts. LabVIEW software for operating the H_2O_2 FIA system was designed by Peter Croot, Maija Heller, Craig Neill and Whitney King. Julián Alberto Gallego-Urrea was supported by a Helmholtz International Fellow Award, 2015 (Helmholtz Association, Germany).

Financial support. This research has been supported by the European Commission, Horizon 2020 Framework Programme (grant no. 603773).

The article processing charges for this open-access publication were covered by a Research Centre of the Helmholtz Association.

Review statement. This paper was edited by S. Wajih A. Naqvi and reviewed by Lanying Ma, Robin Bond, and two anonymous referees.

References

Angel, L. D., Fiedler, U., Eden, N., Kress, N., Adelung, D., and Herut, B.: Catalase activity in macro- and microorganisms as an indicator of biotic stress in coastal waters of the eastern Mediterranean Sea, Helgol. Mar. Res., 53, 209–218, https://doi.org/10.1007/s101520050025, 1999.

Baltar, F., Reinthaler, T., Herndl, G. J., and Pinhassi, J.: Major Effect of Hydrogen Peroxide on Bacterioplankton Metabolism in the Northeast Atlantic, PLoS One, 8, e61051, https://doi.org/10.1371/journal.pone.0061051, 2013.

Bertilsson, S. and Tranvik, L. J.: Photochemically produced carboxylic acids as substrates for freshwater bacterioplankton, Limnol. Oceanogr., 43, 885–895, https://doi.org/10.4319/lo.1998.43.5.0885, 1998.

Bogosian, G., Aardema, N. D., Bourneuf, E. V., Morris, P. J. L., and O'Neil, J. P.: Recovery of hydrogen peroxide-sensitive culturable cells of Vibrio vulnificus gives the appearance of resuscitation from a viable but nonculturable state, J. Bacteriol., 182, 5070–5075, https://doi.org/10.1128/JB.182.18.5070-5075.2000, 2000.

Cho, K., Kasaoka, T., Ueno, M., Basti, L., Yamasaki, Y., Kim, D., and Oda, T.: Haemolytic activity and reactive oxygen species production of four harmful algal bloom species, Eur. J. Phycol., 52, 311–319, https://doi.org/10.1080/09670262.2017.1286525, 2017.

Clayton, T. D. and Byrne, R. H.: Spectrophotometric seawater pH measurements: total hydrogen ion concentration scale calibration of m-cresol purple and at-sea results, Deep-Sea Res. Pt. I, 40, 2115–2129, https://doi.org/10.1016/0967-0637(93)90048-8, 1993.

Cooper, W. J., Zika, R. G., Petasne, R. G., and Plane, J. M. C.: Photochemical formation of hydrogen peroxide in natural waters exposed to sunlight, Environ. Sci. Technol., 22, 1156–1160, https://doi.org/10.1021/es00175a004, 1988.

Cooper, W. J., Shao, C. W., Lean, D., Gordon, A., and Scully, F. E.: Factors affecting the distribution of H_2O_2 in surface waters, Environ. Chem. Lakes Reserv., 237, 391–422, 1994.

Gasol, J. M. and del Giorgio, P. A.: Using flow cytomery for counting natural planktonic bacteria and understanding the structure of planktonic bacterial communities, Sci. Mar., 64, 197–224, https://doi.org/10.3989/scimar.2000.64n2197, 2000.

Gerringa, L. J. A., Rijkenberg, M. J. A., Timmermans, R., and Buma, A. G. J.: The influence of solar ultraviolet radiation on the photochemical production of H_2O_2 in the equatorial Atlantic Ocean, J. Sea Res., 51, 3–10, https://doi.org/10.1016/j.seares.2003.03.002, 2004.

González-Dávila, M., Santana-Casiano, J. M., Petihakis, G., Ntoumas, M., Suárez de Tangil, M., and Krasakopoulou, E.: Seasonal pH variability in the Saronikos Gulf: A year-study using a new photometric pH sensor, J. Mar. Syst., 162, 37–46, https://doi.org/10.1016/j.jmarsys.2016.03.007, 2016.

Granéli, W., Lindell, M., and Tranvik, L. J.: Photo-oxidative production of dissolved inorganic carbon in lakes of different humic content, Limnol. Oceanogr., 41, 698–706, https://doi.org/10.4319/lo.1996.41.4.0698, 1996.

Guillard, R. R. L. and Ryther, J. H.: Studies of marine planktonic diatoms. I. *Cyclotella nana* Hustedt, and *Detonula confervacea* (cleve) Gran., Can. J. Microbiol., 8, 229–239, https://doi.org/10.1139/m62-029, 1962.

Hansel, C. M., Ferdelman, T. G., and Tebo, B. M.: Cryptic cross-linkages among biogeochemical cycles: Novel insights from reactive intermediates, Elements, 11, 409–414, https://doi.org/10.2113/gselements.11.6.409, 2015.

Hansen, H. P. and Koroleff, F.: Determination of nutrients, in: Methods of Seawater Analysis, Verlag Chemie, Weinheim, 159–228, 2007.

Hopwood, M. J., Rapp, I., Schlosser, C., and Achterberg, E. P.: Hydrogen peroxide in deep waters from the Mediterranean Sea, South Atlantic and South Pacific Oceans, Sci. Rep., 7, 43436, https://doi.org/10.1038/srep43436, 2017.

Hopwood, M. J., Riebesell, U., Arístegui, J., Ludwig, A., Achterberg, E. P., and Hernández, N.: Photochemical vs. Bacterial Control of H_2O_2 Concentration Across a pCO_2 Gradient Mesocosm Experiment in the Subtropical North Atlantic, Front. Mar. Sci., 5, 105, https://doi.org/10.3389/fmars.2018.00105, 2018.

Hopwood, M. J., Santana-González, C., Gallego-Urrea, J., Sanchez, N., Achterberg, E. P., Ardelan, M. V., Gledhill, M., González-Dávila, M., Hoffmann, L., Leiknes, Ø., Santana-Casiano, J. M., Tsagaraki, T. M., and Turner, D.: Fe(II) stability in coastal seawater during experiments in Patagonia, Svalbard, and Gran Canaria, Biogeosciences, 17, 1327–1342, https://doi.org/10.5194/bg-17-1327-2020, 2020.

Hughes, C. and Sun, S.: Light and brominating activity in two species of marine diatom, Mar. Chem., 181, 1–9, https://doi.org/10.1016/j.marchem.2016.02.003, 2016.

Keiber, R. J., Zhou, X., and Mopper, K.: Formation of carbonyl compounds from UV-induced photodegradation of humic substances in natural waters: Fate of riverine carbon in the sea, Limnol. Oceanogr., 35, 1503–1515, https://doi.org/10.4319/lo.1990.35.7.1503, 1990.

Kieber, D. J., Miller, G. W., Neale, P. J., and Mopper, K.: Wavelength and temperature-dependent apparent quantum yields for photochemical formation of hydrogen peroxide in seawater, Environ. Sci. Process. Imp., 16, 777–791, https://doi.org/10.1039/c4em00036f, 2014.

Larsen, A., Egge, J. K., Nejstgaard, J. C., Di Capua, I., Thyrhaug, R., Bratbak, G., and Thingstad, T. F.: Contrasting response to nutrient manipulation in Arctic mesocosms are reproduced by a minimum microbial food web model, Limnol. Oceanogr., 60, 360–374, https://doi.org/10.1002/lno.10025, 2015.

Miller, W. L. and Kester, D. R.: Peroxide variations in the Sargasso Sea, Mar. Chem., 48, 17–29, https://doi.org/10.1016/0304-4203(94)90059-0, 1994.

Miller, W. L. and Zepp, R. G.: Photochemical production of dissolved inorganic carbon from terrestrial organic matter: Significance to the oceanic organic carbon cycle, Geophys. Res. Lett., 22, 417–420, https://doi.org/10.1029/94GL03344, 1995.

Moffett, J. W. and Zafiriou, O. C.: An investigation of hydrogen peroxide chemistry in surface waters of Vineyard Sound with $H_2^{18}O_2$ and $^{18}O_2$, Limnol. Oceanogr., 35, 1221–1229, https://doi.org/10.4319/lo.1990.35.6.1221, 1990.

Moffett, J. W. and Zika, R. G.: Reaction kinetics of hydrogen peroxide with copper and iron in seawater, Environ. Sci. Technol., 21, 804–810, https://doi.org/10.1021/es00162a012, 1987.

Moore, C. A., Farmer, C. T., and Zika, R. G.: Influence of the Orinoco River on hydrogen peroxide distribution and production in the eastern Caribbean, J. Geophys. Res., 98, 2289, https://doi.org/10.1029/92JC02767, 1993.

Morris, J. J.: The 'Helper' Phenotype: A Symbiotic Interaction Between Prochlorococcus and Hydrogen Peroxide Scavenging Microorganisms, University of Tennessee, Tennessee, 2011.

Morris, J. J. and Zinser, E. R.: Continuous hydrogen peroxide production by organic buffers in phytoplankton culture media, J. Phycol., 49, 1223–1228, https://doi.org/10.1111/jpy.12123, 2013.

Morris, J. J., Johnson, Z. I., Szul, M. J., Keller, M., and Zinser, E. R.: Dependence of the cyanobacterium Prochlorococcus on hydrogen peroxide scavenging microbes for growth at the ocean's surface, PLoS One, 6, e16805, https://doi.org/10.1371/journal.pone.0016805, 2011.

Morris, J. J., Lenski, R. E., and Zinser, E. R.: The black queen hypothesis: Evolution of dependencies through adaptive gene loss, mBio, 3, https://doi.org/10.1128/mBio.00036-12, 2012.

Morris, J. J., Johnson, Z. I., Wilhelm, S. W., and Zinser, E. R.: Diel regulation of hydrogen peroxide defenses by open ocean microbial communities, J. Plankt. Res., 38, 1103–1114, https://doi.org/10.1093/plankt/fbw016, 2016.

Palenik, B. and Morel, F. M. M.: Dark production of H2O2 in the Sargasso Sea, Limnol. Oceanogr., 33, 1606–1611, https://doi.org/10.4319/lo.1988.33.6part2.1606, 1988.

Petasne, R. G. and Zika, R. G.: Hydrogen peroxide lifetimes in South Florida coastal and offshore waters, Mar. Chem., 56, 215–225, https://doi.org/10.1016/S0304-4203(96)00072-2, 1997.

Price, D., Mantoura, R. F. C., and Worsfold, P. J.: Shipboard determination of hydrogen peroxide in the western Mediterranean sea using flow injection with chemiluminescence detection, Anal. Chim. Acta, 377, 145–155, https://doi.org/10.1016/S0003-2670(98)00621-7, 1998.

Pullin, M. J., Bertilsson, S., Goldstone, J. V., and Voelker, B. M.: Effects of sunlight and hydroxyl radical on dissolved organic matter: Bacterial growth efficiency and production of carboxylic

acids and other substrates, Limnol. Oceanogr., 49, 2011–2022, https://doi.org/10.4319/lo.2004.49.6.2011, 2004.

Redfield, A. C.: On the proportions of organic derivations in sea water and their relation to the composition of plankton, in: James Johnstone Memorial Volume, edited by: Daniel, R. J., University Press of Liverpool, Liverpool, 177–192, 1934.

Reggiani, E. R., King, A. L., Norli, M., Jaccard, P., Sørensen, K., and Bellerby, R. G. J.: FerryBox-assisted monitoring of mixed layer pH in the Norwegian Coastal Current, J. Mar. Syst., 162, 29–36, https://doi.org/10.1016/j.jmarsys.2016.03.017, 2016.

Riebesell, U., Czerny, J., Von Bröckel, K., Boxhammer, T., Büdenbender, J., Deckelnick, M., Fischer, M., Hoffmann, D., Krug, S. A., Lentz, U., Ludwig, A., Muche, R., and Schulz, K. G.: Technical Note: A mobile sea-going mesocosm system – New opportunities for ocean change research, Biogeosciences, 10, 1835–1847, https://doi.org/10.5194/bg-10-1835-2013, 2013.

Rimmelin, P. and Moutin, T.: Re-examination of the MAGIC method to determine low orthophosphate concentration in seawater, Anal. Chim. Acta, 548, 174–182, https://doi.org/10.1016/j.aca.2005.05.071, 2005.

Roe, K. L., Schneider, R. J., Hansel, C. M., and Voelker, B. M.: Measurement of dark, particle-generated superoxide and hydrogen peroxide production and decay in the subtropical and temperate North Pacific Ocean, Deep.-Res. Pt. I, 107, 59–69, https://doi.org/10.1016/j.dsr.2015.10.012, 2016.

Rundt, C.: Organic Carbon Enrichment of Mediterranean Waters: Effects on the Pelagic Microbial Food Web with Emphasis on Microzooplankton Grazing, University of Bremen, Bremen, 2016.

Sanchez, N., Leiknes, Ø., Tsagaraki, T. M., Hopwood, M., Gallego-Urrea, J., Avarachen, M., Kuttivadakkethil, C., Antonio, L., Kankus, J., King, A. L., Reggiani, E. R., Bratbak, G., Larsen, A., Sandaa, R.-A., Egge, J. K., Turner, D., Besiktepe, S., Bizsel, K. C., Bizsel, N., Iriarte, J. L., González, H., Torres, R., Bellerby, R. G. J., Thingstad, T. F., Hoffmann, L., Achterberg, E. P., Vadstein, O., Olsen, Y., and Ardelan, M. V.: Response of the microbial food web to gradients of organic matter and grazing pressure and multi-stressor effect in incubation experiments in three different marine ecosystems: Patagonia, Arctic and Mediterranean, PANGAEA, https://doi.org/10.1594/PANGAEA.911130, 2020.

Schneider, R. J., Roe, K. L., Hansel, C. M., and Voelker, B. M.: Species-Level Variability in Extracellular Production Rates of Reactive Oxygen Species by Diatoms, Front. Chem., 4, 5, https://doi.org/10.3389/fchem.2016.00005, 2016.

Scully, N. M., Cooper, W. J., and Tranvik, L. J.: Photochemical effects on microbial activity in natural waters: The interaction of reactive oxygen species and dissolved organic matter, FEMS Microbiol. Ecol., 46, 353–357, 2003.

Smith, D. C. and Azam, F.: A simple, economical method for measuring bacterial protein synthesis rates in seawater using 3H-leucine, Mar. Microb. Food Webs, 6, 107–114, 1992.

Van Baalen, C. and Marler, J. E.: Occurrence of hydrogen peroxide in sea water, Nature, 211, 951, https://doi.org/10.1038/211951a0, 1966.

Vermilyea, A. W., Hansard, S. P., and Voelker, B. M.: Dark production of hydrogen peroxide in the Gulf of Alaska, Limnol. Oceanogr., 55, 580–588, https://doi.org/10.4319/lo.2009.55.2.0580, 2010.

Voelker, B. M. and Sulzberger, B.: Effects of Fulvic Acid on Fe(II) Oxidation by Hydrogen Peroxide, Environ. Sci. Technol., 30, 1106–1114, https://doi.org/10.1021/es9502132, 1996.

Welschmeyer, N. A.: Fluorometric analysis of chlorophyll a in the presence of chlorophyll b and pheopigments, Limnol. Oceanogr., 39, 1985–1992, https://doi.org/10.4319/lo.1994.39.8.1985, 1994.

Yuan, J. and Shiller, A.: The distribution of hydrogen peroxide in the southern and central Atlantic ocean, Deep-Sea Res. Pt. II, 48, 2947–2970, https://doi.org/10.1016/S0967-0645(01)00026-1, 2001.

Yuan, J. C. and Shiller, A. M.: Determination of subnanomolar levels of hydrogen peroxide in seawater by reagent-injection chemiluminescence detection, Anal. Chem., 71, 1975–1980, https://doi.org/10.1021/ac981357c, 1999.

Zika, R. G., Moffett, J. W., Petasne, R. G., Cooper, W. J., and Saltzman, E. S.: Spatial and temporal variations of hydrogen peroxide in Gulf of Mexico waters, Geochim. Cosmochim. Ac., 49, 1173–1184, https://doi.org/10.1016/0016-7037(85)90008-0, 1985.

Zinser, E. R.: Cross-protection from hydrogen peroxide by helper microbes: The impacts on the cyanobacterium Prochlorococcus and other beneficiaries in marine communities, Environ. Microbiol. Rep., 10, 399–411, https://doi.org/10.1111/1758-2229.12625, 2018.